FATIGUE CRACK INITIATION AND PROPAGATION FROM INCLUSIONS IN STEEL FORGINGS

R.B. Scarlin[o], C. Berger[*], K.H. Mayer[+] and W. Oberparleiter[**]

In order to evaluate the extent to which the presence of inclusions in steel forgings can be tolerated a series of tests has been conducted on specimens containing steel-making inclusions. The results showed that in general crack nucleation occurred at inclusions for which the ΔK value, calculated for a penny-shaped crack of the same area, lay above the threshold value for fatigue crack propagation ΔK_o, in defect-free material. However, a comparison of the distance of fatigue crack propagation with that expected according to linear elastic fracture mechanics shows differences which may be related to the actual irregular shape of the inclusions compared with the assumed circular shape and to the presence of non-uniform stresses.

INTRODUCTION

It is well known that individual non-metallic inclusions and clusters of such defects may still be present in large steel forgings even when using the most modern manufacturing methods. The slow growth of cracks from such defects under non-steady loads, such as may occur during start-up and shut-down of a steam turbine, has led to at least one catastrophic rotor failure (1). For this reason it is necessary to develop a technique which is able to predict whether defects, detected as ultrasonic testing indications, are able to propagate under service loading and at what rate. A fracture mechanics approach has been adopted since a predictive capability is required so that results of laboratory investigations can be applied to the evaluation of defects in large forgings. The aim of the present work has been the development of an engineering approach to the life assessment of fatigue loaded structures containing natural defects. Simplifying assumptions have been made to facilitate the application of fracture mechanics techniques to defects of irregular shape and clusters of defects for which accurate solutions are not available.

It has been shown previously that in the high cycle fatigue range the initiation of cracks from inclusion particles both in a high strength 12% Cr steel (2) and in quenched and tempered low alloy steels (3,4) can be described using linear elastic fracture mechanics, whereby the inclusions behave as though they were cracks of the same size.

+ Maschinenfabrik Augsburg-Nürnberg AG
o BBC Aktiengesellschaft Brown, Boveri & Cie., Baden
* Kraftwerk Union, Mühlheim
** Industrieanlagen Betriebsgesellschaft GmbH, Ottobrunn

In the low cycle fatigue range up to 25,000 cycles pulsating tension tests resulted in crack initiation of the stress intensity amplitude ΔK at a specific inclusion exceeded the threshold stress intensity amplitude ΔK_0 determined using deeply precracked specimens. The aim of the present investigation was the extension of this work to different steels containing other inclusion types both as individual inclusions and as clusters of such defects, whereby particular emphasis was placed on the mechanism of crack initiation and early propagation. The number of loading cycles was limited to 25,000 and the stress levels were maintained below the yield strength in order to simulate the situation arising during start-up and shut-down of power generating equipment.

EXPERIMENTAL PROCEDURE

Two forgings in which large numbers of ultrasonic indications had been recorded were selected for this programme. Details of the manufacturing procedure, component type, defect size and mechanical properties of adjacent, defect-free material are shown in Table 1, whereas the chemical analyses are given in Table 2. The forgings are designated G und H and comprise a 2 CrNiMo steel rotor disc and a creep resistant 1% CrMoV shaft.

Table 3 provides a summary of the results of the ultrasonic tests (equivalent disc reflector ER) along with the findings of the microstructural investigations. The findings may be summarized as follows:

Forging G: grouped irregular defects of $\lesssim 1$ mm ER (silicates)
Forging H: separate and grouped irregular defects of $\lesssim 3$ mm ER (MnS)
Round specimens of diameter 30 mm were machined from the defect-containing regions of the forgings in such a direction that the loading was predominantly normal to the plane in which the defects lay. The specimens were then subjected to pulsating tension loading (ratio of minimum to maximum load R of 0.1) for up to 25,000 cycles at room temperature or until potential drop measurements indicated that significant crack growth had occurred. The experimental setup is shown in Fig. 1. Various stress amplitudes were used from a lowest value of 60% of the yield strength upto values at which the maximum stress approached the yield strength. After termination of the fatigue loading experiments the specimens were cooled in liquid nitrogen and broken open in a brittle manner. The fracture surfaces were examined in the optical and scanning electron microscope for evidence of the inclusions and nucleated fatigue cracks. Particular attention was paid to evidence of interaction between defects. At higher magnification the fatigue crack regions could be clearly identified and distinguished from the surrounding brittle overload failure.

In forging G the silicate inclusions (Fig. 2) posses a complex shape with irregular arms but appear essentially as independent defects even though the ultrasonic test indicated closely spaced particles. Since the separations between individual defects are larger than the defects themselves no interaction will be expected in the early stages of crack propagation (5)and the inclusions will be considered separately. However, certain of the MnS inclusions in forging H lie in close proximity to one another so that they had to be evaluated together in considering their ability to nucleate fatigue cracks. The MnS inclusions appeared either as blocky (Fig. 3) or irregular dendritic particles (Fig. 4).

Chemical composition of the inclusions was confirmed using an X-ray diffractometer in the scanning microscope. For all forgings it was possible to observe flaws at which fatigue cracks had nucleated and other present in the brittle overload region but at which no crack had nucleated during fatigue loading. The fracture mechanics evaluation was performed in the following way:

> For individual non-interacting defects (all inclusions in forging G and some of these in forging H) the area of the irregular inclusion was determined using a planimeter and the radius of the circle, a, with the same area was calculated.
>
> For groups of interacting defects (certain clusters in forging H) the separate inclusion areas were measured, added together and again the radius of the circle, a, with the same total area was determined.

The stress intensity amplitude ΔK is then calculated from a, the effective crack radius for an embedded defect or the effective crack depth for a surface defect, using the following formulae:

$$\Delta K = \Delta\sigma \cdot \sqrt{\frac{\pi \cdot a}{Q}} \quad \text{for an embedded defect}$$

$$\text{or } \Delta K = \Delta\sigma \cdot \sqrt{\frac{1{,}21 \cdot \pi \cdot a}{Q}} \quad \text{for a surface defect}$$

where $\Delta\sigma$ is the applied stress amplitude and Q is the appropriate shape factor for a (semi) circular crack.

These ΔK-values were then compared with ΔK_0, determined at the same R-value on compact tension specimens taken in the same orientation from adjoining defect-free regions of the same forgings. The ΔK_0-values were carefully determined by small incremental step decreases of the loading amplitude while monitoring the crack with the potential drop technique. On the basis of fracture mechanics, i.e. if the inclusion areas behave as sharp cracks, fatigue cracking would be expected at all flaws for which ΔK lies above ΔK_0.

RESULTS AND DISCUSSION

In the following the subjects of crack initiation and of crack propagation will be examined in turn. Reasons for discrepancies between the fracture mechanics predictions and the actual observations will be sought in the simplifying assumptions made in the fracture mechanics analysis and in the material behaviour itself which does not comply with the implicit expectation of homogeneous behaviour.

Crack initiation criterion

The results of the evaluation of the fracture surfaces with respect to crack initiation are shown in Fig. 5. Inclusions were examined on the fracture surfaces of the specimens taken from the 2 forgings. In each case the ΔK-values are plotted with open points indicating flaws at which no fatigue crack had nucleated and closed points showing those at which cracking was observed. Triangles mark surface defects and circles embedded ones.

In addition a letter c adjacent to the symbol refers to a defect cluster where a single ΔK-value was calculated for a number of neighbouring flaws. The measured ΔK_o-values are shown on the same diagram and correspond to a propagation rate of 2×10^{-10} m/cycle. This corresponds to a distance of 5 mm at a magnification of 1000 x in the scanning microscope related to 25000 cycles testing - the lower detection limit for the presence of a small fatigue crack. A scatterband of ± 10% has been added to the ΔK_o-values to account for the observed variability within the forgins tested.

A clear-cut case is provided by forging 'G' containing silicate inclusion areas (All are irregular individual flaws). In this case fatigue cracking is observed at all inclusions for which $\Delta K > \Delta K_o$ and at the only inclusion for which $\Delta K < \Delta K_o$ no fatigue crack was observed. Apparently the brittle fracture path is less likely to pass through uncracked silicate inclusion areas.

Turning now to the results from forging "H", which contained solely fine irregular MnS inclusions, sometimes in association with pores, it is apparent that, although fatigue cracks are observed in all cases for ΔK above the ΔK_o-range and the absence of fatigue cracks is only observed below ΔK_o, some inclusions slightly below and at the bottom edge of the ΔK_o-band show considerable amounts of fatigue cracking. This is almost exclusively the case for defect clusters so that a discrepancy in the analysis may arise from the method used for the calculation. In such cases the individual inclusion areas lying in close proximity to oneanother have been added together and ΔK calculated for a circle of size equal to the summed areas. A recent publication (6) has indicated that this may underestimate the effective stress intensity amplitude at the points of nearest approach of the adjacent defects. The subjects of closely spaced defects and of areas in which the inclusion particles are nonuniformly distributed are dealt with in more detail in another publication (7).

It is apparent, at least in the case of individual inclusions that simple fracture mechanics methods involving a comparison of the specific ΔK-value with ΔK_o permit a prediction of the ability of an inclusion particle to initiate a fatigue crack. However no evaluation of the propagation rate in comparison with that of a sharp crack, or of the possibility that a number of fatigue cycles may be required to initiate a crack (incubation time) has as yet been made.

Mechanism of fatigue cracking

For both forgings the process and morphology of fatigue crack development and growth from the inclusions was followed in detail by examining the shape and size of the fatigue cracked areas. Examination of inclusions of different size (and initial ΔK-value) shows an increasing extent of crack development for larger sizes. By observing different inclusions in forging H it can be seen that the cracks nucleate at points between the irregular arms of irregular-shaped inclusions (Fig. 6) and propagate locally around the periphery until they meet and are able to break free from the inclusion first at the position of the smallest inclusion width (minor axis of ellipse, Fig. 7), with further development towards a circular shape until the crack separates completely from the inclusion. This observation is in line with considerations of the variation of the stress intensity factor around the periphery of elliptical cracks. The same applies to defects at or near the specimen surface resulting in the formation of a semicircular surface crack (Fig. 8).

Crack propagation behaviour

A comparison was made between the observed extent of crack propagation and that which would be expected for an ideal circular crack with the same area as the irregularly shaped inclusion area. Since the area of crack propagation, at least in the early stage, i.e. for small inclusions, is local and irregular it was determined along with that of the inclusion using the planimeter and again converted to a circle of equivalent area. The observed crack growth ($\Delta a_{obs.}$) is now given by the linear increase in radius of the equivalent circle as a result of fatigue cracking. This was then compared with the linear increase in size expected for a circular crack having the same area as the inclusion (Δa_{calc}) by integration of the fatigue crack growth curve measured with compact tension specimens, taken from defect-free regions of the same forgings. The integration of the fatigue crack growth rate, da/dN, was performed using the equation:

$$\frac{da}{dN} = C \quad (\Delta K^n - \Delta K_o^n)$$

whereby C and n were determined by fitting to the Paris-section of the curve and ΔK_o is the threshold value. The integration was performed in steps of 100 cycles. The results of the comparison are shown in Fig. 9 for forging G and Fig. 10 for forging H as a function of the initial ΔK-values obtained by equating the inclusions to circular cracks of the same area. Each inclusion which nucleated a fatigue crack provides one point on the diagram. A ratio of Δa_{obs} to Δa_{calc} of unity would indicate that linear elastic fracture mechanics had correctly predicted the observed extent of cracking.

Fig. 9 shows the results for forging G, the 2 % Cr Ni Mo steel, which contains irregular silicate inclusions with measured equivalent radii in the range 0.14 to 0.56 mm. It is apparent that an approach to ideal fracture mechanics behaviour, i.e. $\Delta a_{obs}/\Delta a_{calc} \approx 1$ is only observed at the very small defects. Larger inclusions show less crack growth than the simplified fracture mechanics method predicts. In order to make a comparison the results obtained by Elsender et al (4) on a 3.5 % Ni Cr Mo V steel which contained alumino-silicate inclusions have been reanalysed and also plotted on Fig. 9. A similar tendency can be seen, the ratio of observed to calculated crack growth again exceeds unity only at small inclusion sizes (small initial ΔK) and reduces also the value below 0,3 for the larger inclusions i.e. for larger amounts of crack extension. The agreement with the present results cannot be considered fortuitous. However Fig. 10 which presents the crack growth results at the MnS inclusions in forging H, a 1 % Cr Mo V steel, is in marked contrast. The inclusions have equivalent radii in the range 0.07 to 0.32 mm. Although the ratios of observed to calculated crack growth are again highest for the smallest inclusions, they show values in excess of 200 for small inclusions and a reduction towards unity where greater amounts of cracking have occured. The data points marked with a letter "c" are again for inclusion clusters, in which interaction is observed. Only crack growth at embedded defects, which is the case of major practical interest, has been analysed for the two forgings, since a quantitative evaluation of near-surface or surface intersection defects is inaccurate as a result of changes in crack shape.

Since we are not dealing with an idealised system but rather with one in which many complications arise it must be realised that the discrepancy between the observed extent of crack propagation and that predicted by

linear elastic fracture mechanics may arise from one or more of a number of assumptions, such as that:

- The inclusions behave as sharp cracks, i.e. no incubation time is required
- The behaviour of these irregular shaped cracks is the same as that of circular cracks of the same area and the interaction of closely spaced inclusions can be accounted for by the summation procedure described above.
- The material is uniform with respect to properties (e.g. Youngs modulus) and stresses within both the matrix and inclusion particle.
- The growth behaviour of short cracks in the vicinity of the inclusion particles may be equated to that of long crack in fracture mechanics specimens.

These factors will be considered in turn.

Incubation time

Further insight into the presence or otherwise of an incubation time can be obtained by a comparison of the actual number of loading cycles applied to each specimen (N_{test}) with the number of cycles which an integration of the crack growth rate curve indicates would be necessary for the observed amount of crack propagation (N_{calc}). The determination of N_{calc} assumes implicity that no incubation time is required. The following cases may be distinguished

$N_{test} > N_{calc}$ implies an incubation time may be present

$N_{test} = N_{calc}$ indicates that fracture mechanics (and the assumptions made in the analysis) has made an accurate prediction.

$N_{test} < N_{calc}$ means that cracking is faster than predicted.

Fig. 11 shows that whereas inclusions in forging G show less crack growth than would be expected from a crack of equivalent size the opposite is true for forging H.

These observations are consistent with the postulate that an incubation time is required for initiation of fatigue cracks at silicate inclusions in forging G but not at MnS inclusions in forging H. This behaviour could also result from non-uniform stress fields which will be present as a result of differences in Young's modulus. Such stresses would affect both the initiation and propagation rate.

It should be noted that the presence or absence of an incubation time will not affect the validity of the ΔK vs. ΔK_o comparison shown in Fig. 5, since this diagramm considers only the presence or absence of a crack and not the extent of growth which is the factor most affected by an incubation time.

Irregular crack shape/short cracks

Since stress intensity factors are not available for irregularly shaped defects, circular cracks of the same projected area have been considered. This was necessary despite the fact that it has been shown (8, 9) that the K-value at the points of intersection of overlapping elliptical cracks greatly exceed those at a circle of equivalent area, so that the effective crack driving force at these locations is very high, consistent with their being the preferred crack initiation points. This factor will tend to result in earlier local crack initiation at more irregularly shaped inclusions. Although the summation procedure for closely spaced inclusions in a cluster is not based on any physical model of crack growth it yields results, as shown in Fig. 10, which are comparable with those for the individual defects in the same figure. In addition it is now well established that short cracks, i.e. cracks which are small in comparison with metallurgical features such as the grain size or martensite lath width exhibit higher growth rates than long cracks at the same ΔK-value. This will accelerate cracking rates at crack lengths of less than ca. 0.1 mm. This will apply only at the very smallest measured crack sizes (10).

Uniformity of properties and stresses

Of particular interest are differences in properties between the inclusion and the matrix which will lead to non-uniform stress fields during service loading, in particular coefficient of thermal expansion (α) and Young's modulus (E). As a result of the higher α-value of MnS than the matrix and lower α-value of silicates (12) than the matrix after cooling from the heat treatment to room temperature, tensile stresses will arise in the MnS particles and compressive stresses in the silicates. Since the bonding of MnS particles to the matrix is relatively weak, decohesion or even cracking could occur which will relax the stresses in the adjoining matrix to low values. However the compressive stresses will remain within the silicate particles resulting in significant tensile stresses in the surrounding matrix. These constitute residual stresses present before fatigue loading is performed.

When tensile stresses are applied during the fatigue cycle the difference in Young's modulus between inclusion and matrix will lead to non-uniform mechanical loading. Since the silicates in forging G have a higher Young's modulus than the matrix, the local stress in the matrix will be reduced as a result of the higher stress level in the inclusion. This reduced matrix stress level will be superimposed on the tensile stress resulting from thermal expansion and will determine the local propagation rate of cracks in the early stages. Fig. 9 shows that the observed growth rates adjacent to silicate particles are significantly lower than predicted on the assumption that stress fields are uniform.

The converse is true for the MnS inclusions in forging H: In this case the inclusion has a lower Young's modulus than the matrix (11). The effective stress level in the matrix adjacent to the inclusion will be higher than in the absence of the inclusion particle so that crack propagation rates will be higher than predicted on the simple fracture mechanics basis. This could provide at least a partial explanation for the very large amounts of crack propagation observed adjacent to inclusions in forging H and shown on Fig. 10. It is expected that these non-uniform stress fields will reduce rapidly with increasing distance from the inclusion (inversely proportional to the third power of the distance

from the inclusion centre). This implies that the accelerating or retarding effect of local non-uniform stress fields will only be observed for relatively small amounts of cracking. It is also true that for very large amounts of crack propagation any effects of incubation times or growth in local non-uniform stress fields will become negligible and the overall behaviour will conform with the predictions of linear elastic fracture mechanics.

Fig. 12 summarises the various factors which affect the crack propagation rate. Whereas at the very smallest crack sizes high growth rates are expected in all cases, at intermediate stress intensity values higher growth rates than predicted using fracture mechanics will be observed only at inclusions with a lower Young's modulus than the matrix (sulphides). It is expected that the predictions of linear elastic fracture mechanics will be accurate when large amounts of crack propagation have occured, i.e. Fig. 8.

CONCLUSIONS

The results of the present investigation indicate the success of a simple engineering approach to the problem of initiation and propagation of fatigue cracks from inclusions commonly present in large steel forgings. An approximation of actual inclusions of irregular shape to a circular crack of the same area and a comparison of the resulting stress intensity amplitude with the threshold value for the propagation of cracks in defect-free material provides a good prediction of the ability of inclusions to provide nucleation sites for fatigue cracks.

However the extent of crack propagation observed can differ considerably from that expected from a fracture mechanics analysis made using various simplifying asumptions. The discrepancy probably arises from the effect of inhomogeneous stress fields generated adjacent to the inclusion particles as a result of differences in Young's modulus in combination with the necessary simplification of treating actual irregular inclusions as regular circular cracks.

ACKNOWLEDGEMENTS

The authors would like to express their thanks to the Forschungsvereinigung für Verbrennungskraftmaschinen for the provision of finances to perform a major part of the work, to the Industrieanlagen Betriebsgesellschaft mbH (IABG) where the tests were carried out and especially to the members of the advisory group which provided invaluable help during the course of the work.

REFERENCES

1. Kramer,L.D., "Analysis of the Tennessee Valley Authority", Gallatin Unit No. 2 turbine rotor burst; presented at the winter annual meeting of the American Society of Mechanical Engineers (New York, December 5 - 10, 1976)

2. Friedl,K.H., Scarlin,R.B. and Zelizko, V., "Advances in Fracture Research", ICF5 (29 March - 3 April 1981, Cannes, France) Vol. 2, p. 923.

3. Harkegard,G., Eng. Fract. Mech., 6, (Dec. 1974) 795.

4. Elsender,A., Gallimore,R. and Poynton,W.A., Fracture 1977, ICF4, (June 19 - 24, Waterloo, Canada) Vol.2, p. 953.

5. Melville,R.H., "Conference on Fracture Mechanics in Engineering Practice", (Sheffield, Sept. 1976) CEGB Report LM/MATS/098

6. Phang,Y. and Ruiz,C., "Conference on Application of Fracture Mechanics to Materials and Structures", (June 20 - 24, 1983, Freiburg, Germany, Proceedings in press)

7. Berger,C., Mayer,K.H., Oberparleiter,W. and Scarlin,R.B., ICF6, (Dec. 1984, New Dehli, in press)

8. Gruter,L. and Huget, G., "Proceedings of 13 th Meeting of Fracture Group" (6 - 7 Oct. 1981, Hannover, Germany) p. 55 - 62

9. Oore,M. and Burns,D.J., Trans. ASME 102 (1980) p. 202 - 211

10. Ritchie,R.O. and Suresh,S., "Mechanics and Physics of the Growth of Small Cracks", In. Symp. on Short Crack Behavior, (Toronto, 1982), to be published.

11. Eid,N.M.A. and Thomson,P.F., Acta Metallurgica 27 (1979), p. 1239 - 49

12. Brookbank,D. and Andrews,K.W. Journal of the Iron and Steel Institute, 210 (1972) 4, p. 246 - 255.

Table 1: Descriptions of the forgings and their mechanical properties

	Material	Forging	Dimensions	Melting procedure 1)	Ingot weight MPa	0,2 Proof strength MPa	Impact energy 20^{o} J	FATT 50 ^{o}C
G	23CrNiMo747	Disc	Ø1720 x 620	EL and CAP	12	660	98	+ 5
H	21CrMoV5 11	Shaft	Ø1150,Ø300x1100	EL	-	640	62-70	+ 50

Table 2: Chemical composition of the forgings in%

	Material	C	Si	Mn	P	S	Al	Cr	Mo	Ni	V
G	23CrNiMo747	0,23	0,09	0,74	0,014	0,009	0,003	1,80	0,72	1,07	0,05
H	21CrMoV5 11	0,23	0,31	0,37	0,010	0,009	0,007	1,29	0,97	0,24	0,26

Table 3: Microstructure and defect types

Forging	Defect category ER 1)	Microstructure	Grain size ASTM	Defect type	Geometrical form
Disc G	C 1 mm	Bainite and Martensite	3 - 4	small density packed Calcium-Aluminium-Silicate particles	irregular equiaxed or elongated
Shaft H	I and C 3 mm 2)	Ferrite and Pearlite	7 - 8	MnS particles (type II and III) also associated with pores	dendritic and compact irregular, approx. equiaxed

1) ER - Equivalent disc reflector 2) I - individual defect
C - defect cluster

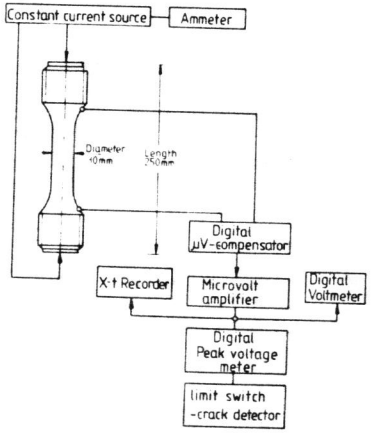

Fig 1 Experimental testing arrangment

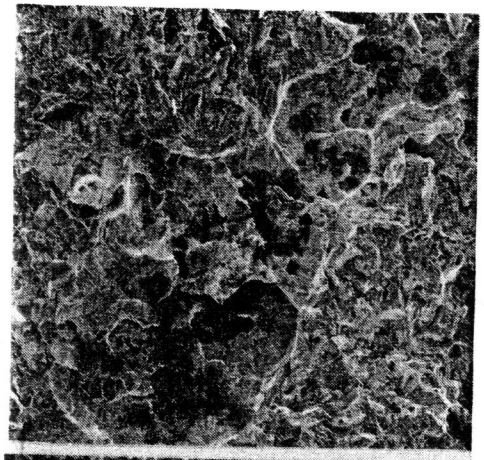

Fig. 2:
silicate inclusion with irregular arms in forging G

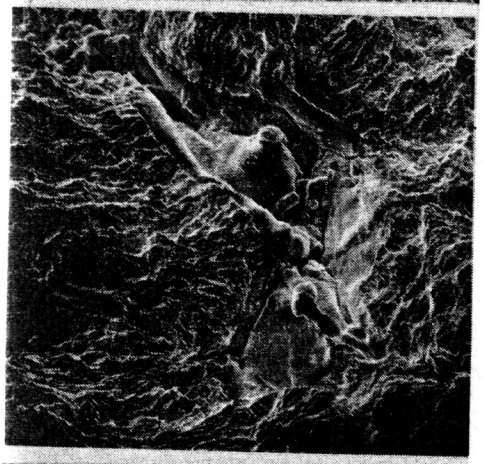

Fig. 3:
blocky Mn S-inclusion in forging H

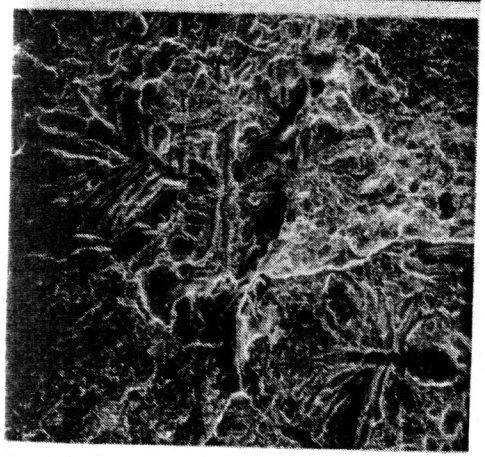

Fig. 4:
dendritic Mn S-inclusion in forging H

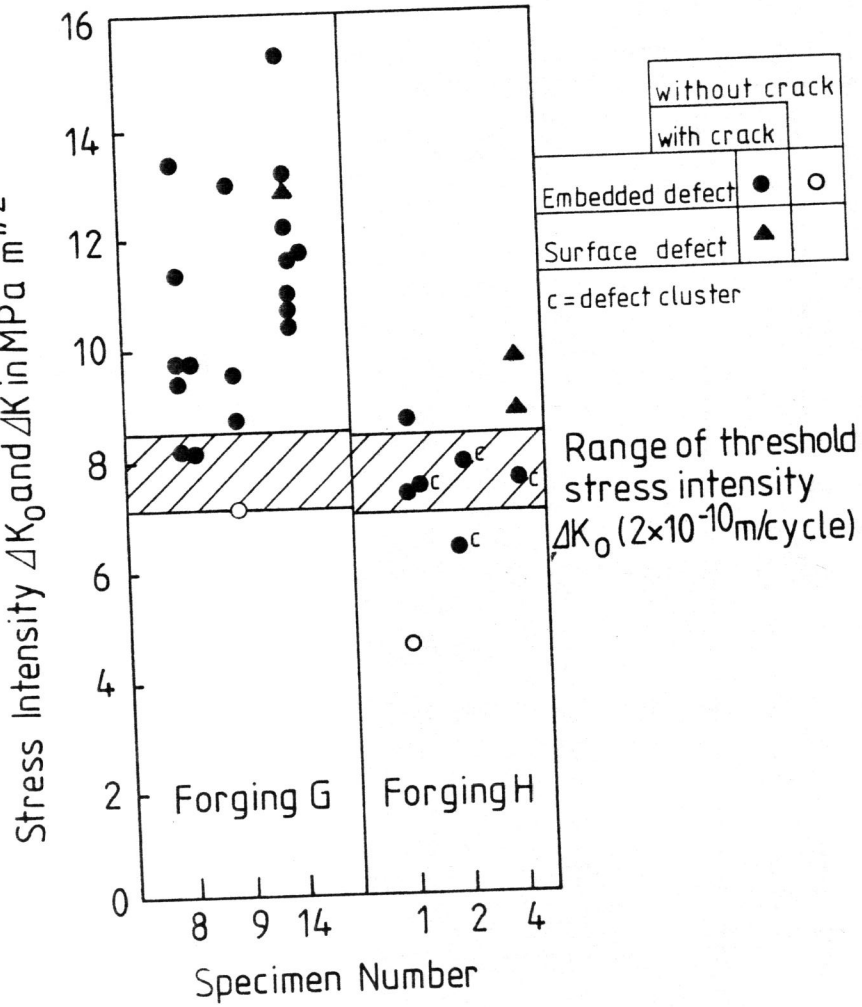

Fig. 5: Comparison of calculated ΔK values with measured threshold ΔK_o

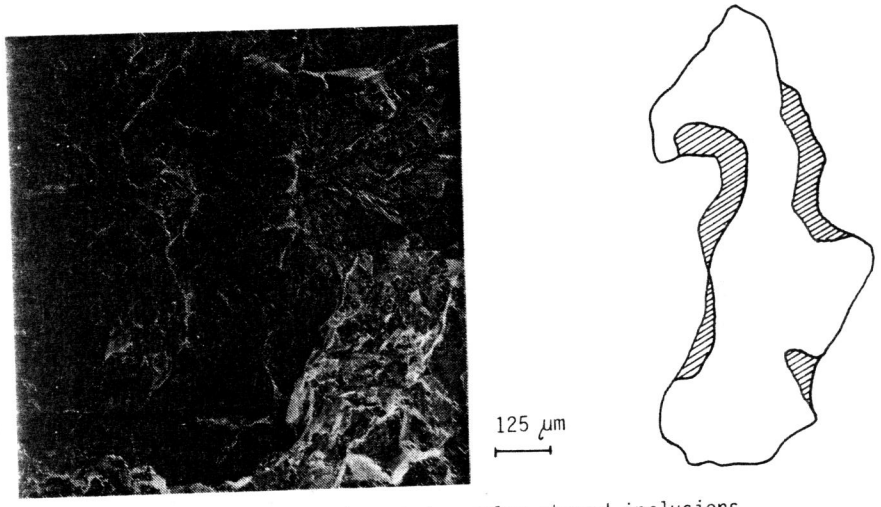

Fig. 6: local crack nucleation at irregular shaped inclusions

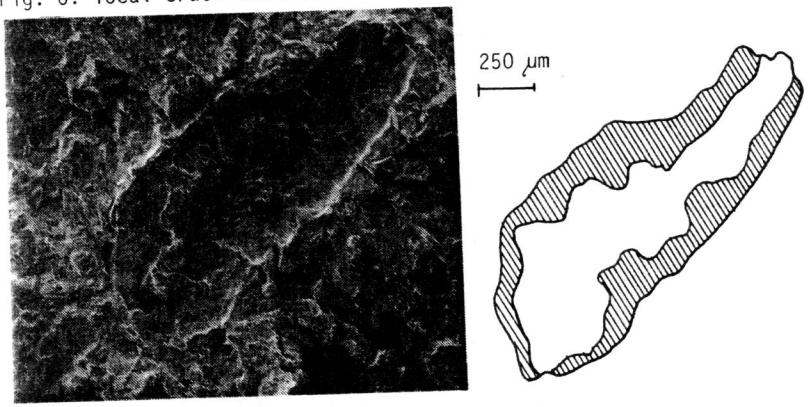

Fig. 7: closed crack front around the inclusion

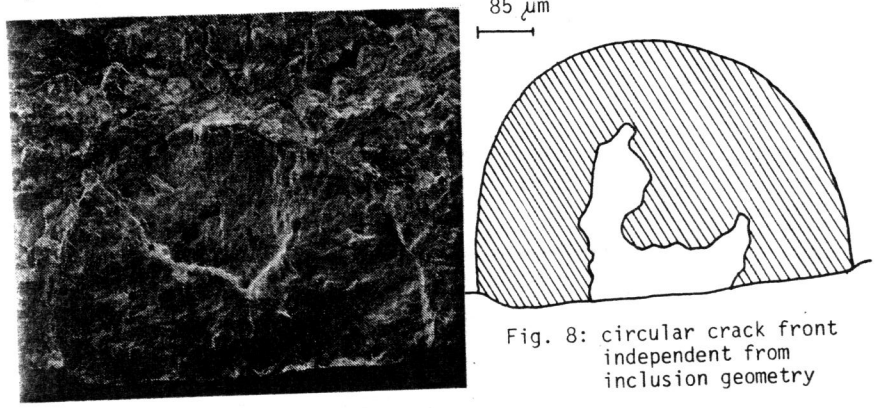

Fig. 8: circular crack front independent from inclusion geometry

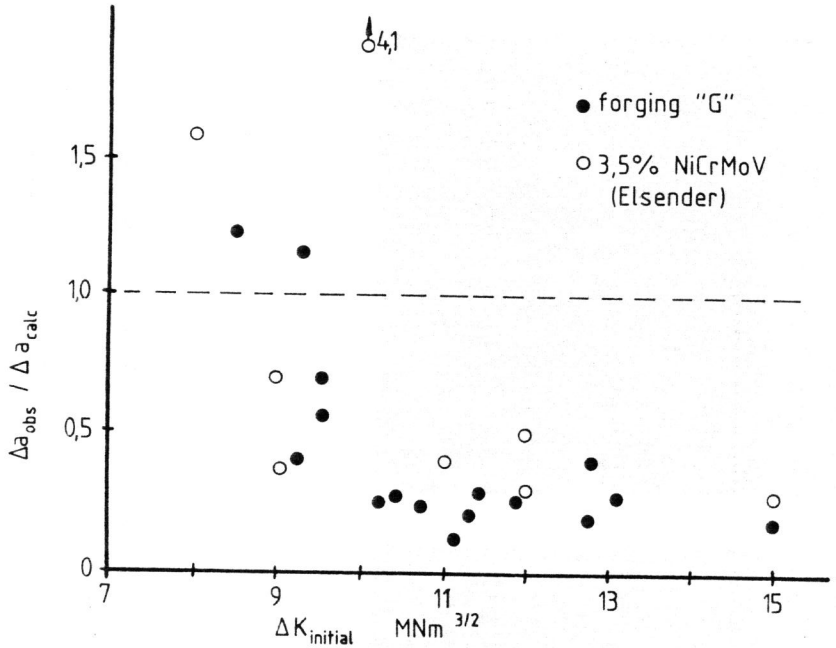

Fig. 9: Ratio of observed to calculated crack propagation as a function of initial ΔK - forging G

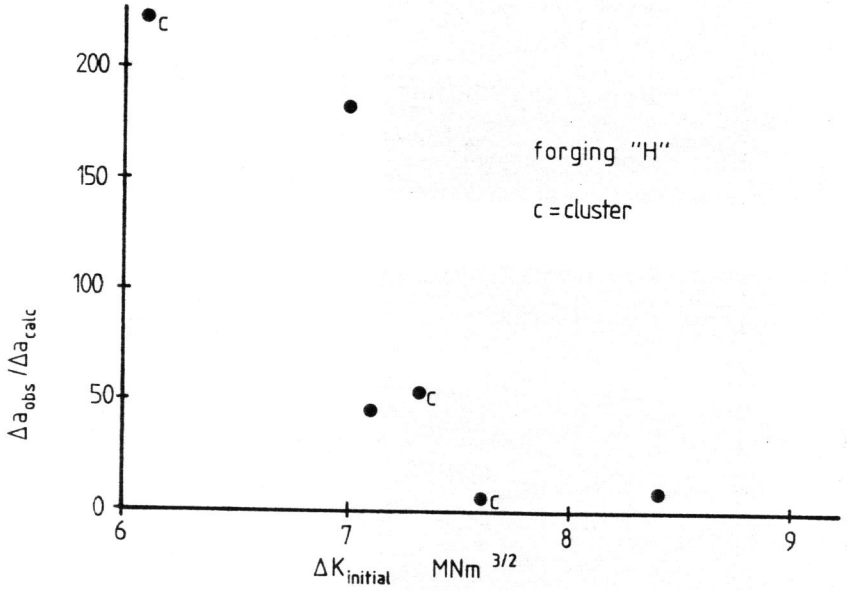

Fig. 10: $\Delta a_{abs}/\Delta a_{calc}$ vs. initial ΔK - forging H

Fig. 11: Comparison of the actual number of loading cycles N_{test} in fatigue test with the number of cycles calculated according to fracture machanics considerations N_{calc} for the observed extent of crack propagation

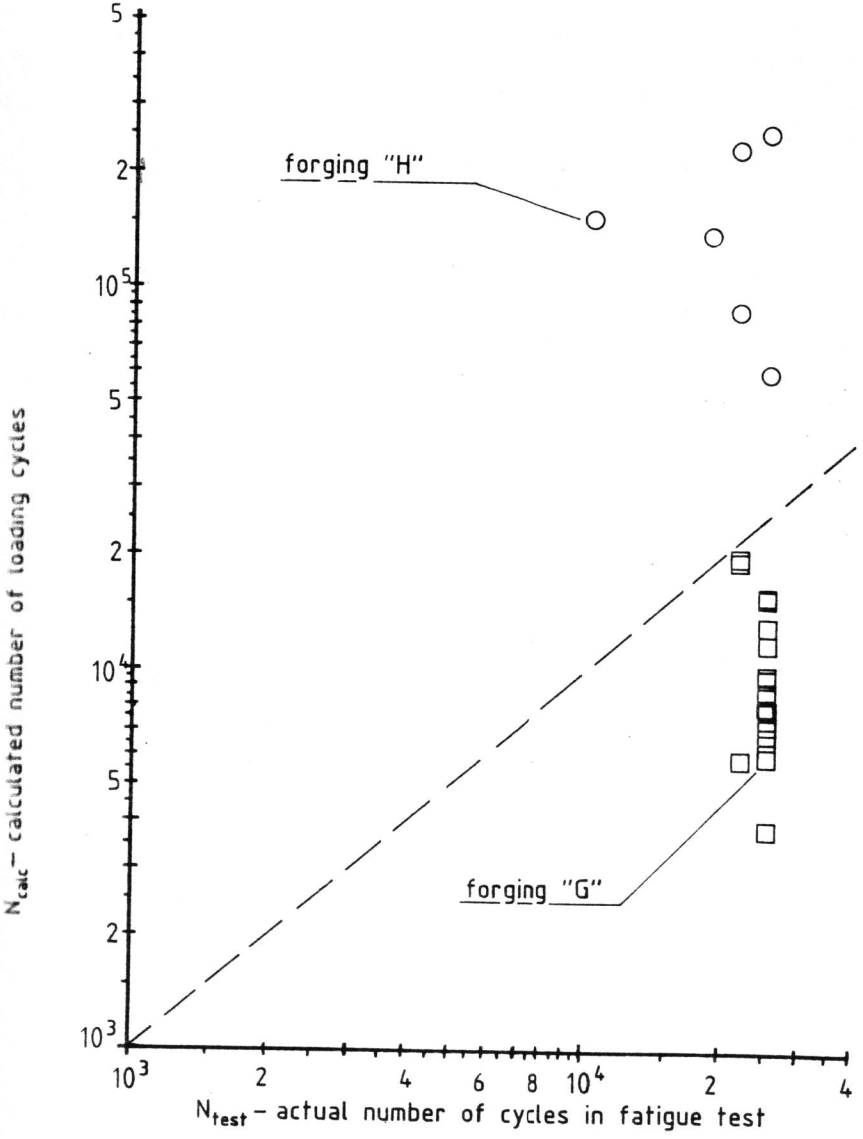

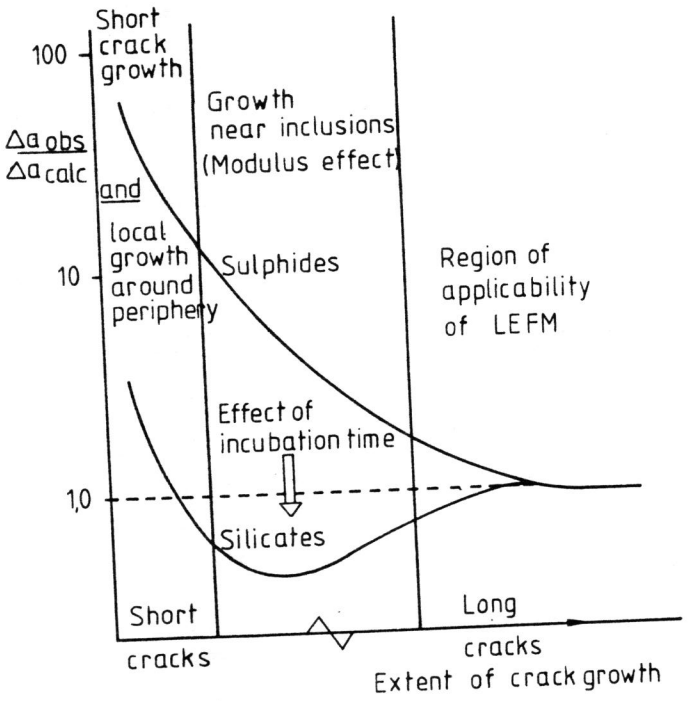

Fig. 12: Schematic representation of observed and calculated extent of crack propagation from inclusion particles.